

Archived at the Flinders Academic Commons

<http://dspace.flinders.edu.au/dspace/>

Copyright (2005) American Institute of Physics. This article may be downloaded for personal use only. Any other use requires prior permission of the author and the American Institute of Physics.

The following article appeared Curran, S., Ellis, A.V., Vijayaraghavan, A., & Ajayan, P.M., 2004. Functionalization of carbon nanotubes using phenosafranin. *Journal of Chemical Physics*, 120(10), 4886-4889. *and may be found at* [doi:10.1063/1.1644109](https://doi.org/10.1063/1.1644109)

Functionalization of carbon nanotubes using phenosafranin

S. A. Curran^{a)}

*Department of Physics, New Mexico State University, Las Cruces, New Mexico 88001
and Nanotechnology Center, Rensselaer Polytechnic Institute, Troy, New York 12180*

A. V. Ellis^{b)}

*Department of Physics, New Mexico State University, Las Cruces, New Mexico 88001
and Material Science and Engineering Department, Rensselaer Polytechnic Institute, Troy, New York 12180*

A. Vijayaraghavan^{c)} and P. M. Ajayan^{d)}

Material Science and Engineering Department, Rensselaer Polytechnic Institute, Troy, New York 12180

(Received 1 August 2003; accepted 3 December 2003)

Spectroscopic analysis and atomic force microscopy (AFM) phase imaging studies show self-assembly of phenosafranin (PSF) to multiwalled carbon nanotubes (MWNTs). The shift in absorption spectra is associated with charge transfer of valence electrons from PSF to electron accepting sites on the MWNTs. The Raman-active disorder modes are used to fingerprint PSF attachment to MWNTs via defect states. AFM phase imaging was used to obtain a molecular topographic visual confirmation of PSF attached to the MWNT. © 2004 American Institute of Physics. [DOI: 10.1063/1.1644109]

For the last decade scientists in the fields of physics, chemistry, and material science have wondered at the electronic and optoelectronic properties of macromolecular structures, such as fullerenes and carbon nanotubes, and in particular the application of these properties to these fields. From the initial discovery of multiwalled nanotubes (MWNTs) to the revelation of helicity in single-walled nanotubes (SWNTs), we have been amazed that such a seemingly simple construct should have so many varied properties.^{1–3} However, the key factor to carbon nanotubes (CNTs) is that they possess unblemished conjugation with insulating, semi-conducting, or metallic properties, stability in air, and do not require chemical doping to retain such properties. The first indication that combining other organic molecules to carbon nanotubes, forming a unique composite, was carried out using PmPV with MWNTs, resulting in higher than expected enhanced physical properties of the composite.⁴ Since then, many studies have been carried out to alter the chemistry of CNTs in order to tailor its properties to specific requirements, very much in a similar manner to polyacetylene manipulation which has resulted in many unique optoelectronic and molecular switching organic materials.⁵

Assembly of various materials either electrostatically,⁶ hydrophobically,⁷ or covalently^{8,9} onto the surface of CNTs is of great interest in that they dramatically enhance the potential of nanotubes to be used as devices such as single-electron transistors,^{10,11} molecular diodes,^{12–14} memory elements,¹⁵ logic gates,^{16,17} and nanoscale low Ohmic metallic contacts.¹⁸ In addition, depending on the catalytic appli-

cation, various metals^{19,20} or metal complexes^{21,22} can be tethered to the nanotube template.^{23–25} Tethering optically active species such as quantum dots^{22–26} can harness their resonant tunneling effects to make nanodevices for optical applications. Recent work by Zhang and co-workers²⁷ has shown that the adsorption of anthracene derivatives to SWNTs occurs through a donor–acceptor charge-transfer interaction. This form of interaction has also been seen upon attachment of aniline to SWNTs (via formation of an adduct).²⁸

Here we report a unique approach to the adsorption of a cationic phenazine dye, phenosafranin (PSF), at defect sites induced by acid treatment of MWNTs. PSF was chosen for several reasons: (a) Phenazine dyes have great potential for use in solar cells—for example, coupled with EDTA generates photovoltages of 600 mV.²⁹ In addition, PSF can undergo reversible reduction with long-lived excited states which make them ideal as photosensitizers in energy and electron transfer reactions.³⁰ (b) Its amine functionalities may make it more easily dispersible in Nylon 6 for future polymer composite work.

MWNTs synthesized by the arc-discharge method were first purified by sonication in conc. 70/30 H₂SO₄/HNO₃ in an ultrasonic bath for 6 h. The tubes were then filtered through a Whatman nylon microfilter, 0.20 μm, and washed with de-ionized water. This method of chemical functionalization creates dangling bonds that are progressively oxidized depending upon the intensity of treatment to hydroxyl (–OH), carbonyl (>C=O) and carboxyl groups (–COOH).^{19,23} Synthesis of phenosafranin (3,7-diamino-5-phenylphenazine or PSF) functionalized MWNTs (Fig. 1) was achieved by mixing 3 mg of carboxylated nanotubes in 5 ml of de-ionized water containing 0.1% v/v PSF.

After mixing the solution was sonicated for 1 min. While the carboxylated tubes appeared soluble in de-ionized water,

^{a)} Author to whom correspondence should be addressed.

FAX: 001-505-6461934.

Electronic mail: shay@physics.nmsu.edu and drshaycurran@eircom.net

^{b)} Electronic mail: aellis@nmsu.edu

^{c)} Electronic mail: vijaya@rpi.edu

^{d)} Electronic mail: ajayan@rpi.edu

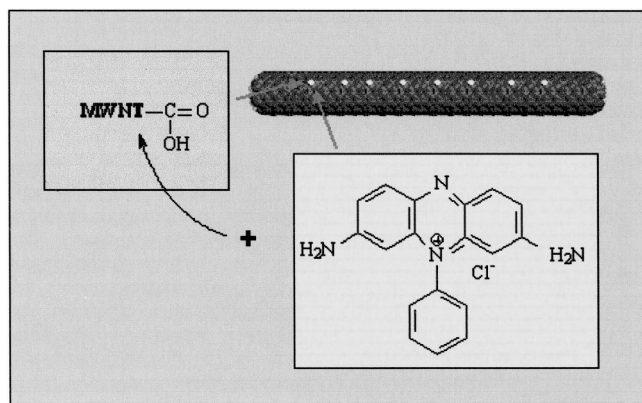


FIG. 1. Charge transfer complex formation between carboxylated multi-walled carbon nanotubes (MWNTs) and phenosafranin (PSF).

after the addition of the PSF there is a notable change in their solubility as the nanotubes segregate from the solution, a clear indication of PSF attachment. The product was filtered under vacuum through a 0.2- μm nylon microfilter and washed thoroughly with de-ionized water, then air dried and stored in a desiccator.

Samples were analyzed spectroscopically using a Varian Cary 500 Scan UV-vis-NIR spectrophotometer to obtain UV-visible absorption spectra from suspensions of samples in water placed in a quartz cell with a path length of 1 cm. Raman spectra were obtained using a Renishaw Ramascope Raman spectrometer equipped with an intergral Leica (DMLM) microscope. A 514.5-nm radiation was produced from a 20-mW air-cooled Ar^+ laser (Spectra-Physics model 263C). The Raman band of silicon, 520 nm, was used to calibrate the spectrometer, with a resolution better than 1.5 cm^{-1} . A Digital Instruments multimode scanning probe microscope with a quadrex extendor module was used to image the nanotubes and dye attached nanotubes.

Shown in Fig. 2 are the UV-visible spectra of pristine MWNTs, acid-treated MWNTs, and acid-treated MWNTs after PSF dye attachment. Notably, Mie scattering is observed after acid treatment of the tubes (cf. pristine tubes), characterized by the rapid increase in base line at decreasing wavelengths. This phenomenon is caused by the acid treatment creating shortened tubes of similar length scales and electrical characteristics such that they can separate or disperse different wavelengths (read colors) of light.

The absorption maximum for PSF is at 520 nm (2.38 eV) while the absorption maximum for the broadband of PSF treated carboxylated nanotubes is 562 nm (2.21 eV), a shift of 0.17 eV (Fig. 2). This bathochromic or redshift clearly indicates chemisorption, primarily due to the phenosafranin-MWNT interaction which allows excitation transfer (caused by light) from the phenosafranin dye to the nanotube and vice versa.³¹ This would indicate that the bond formation or charge transfer process is far stronger than a simple electrostatic process. Carbon nanotubes, in general, are believed to be good electron acceptors.³² In this case the dye has attached to the nanotube; the result is that there is a drop in the dye molecules highest occupied and lowest unoccupied molecular orbital (HOMO-LUMO) gap due to the

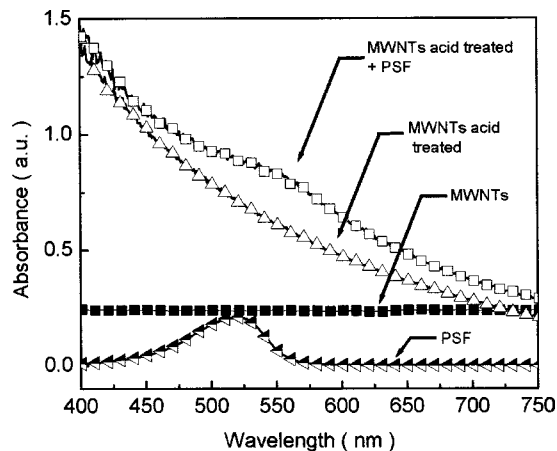


FIG. 2. UV-visible absorption spectra of \blacktriangleleft phenosafranin (PSF), \blacksquare pristine multiwalled carbon nanotubes (MWNTs), \triangleleft multi-walled carbon nanotubes (MWNTs) acid treated, and \square multiwalled carbon nanotubes (MWNTs) acid treated+phenosafranin (PSF).

electron transfer process. Consequently, a decrease in vibrational freedom inflicted by the new charge transfer process takes place as valence electrons are transferred from the PSF attached molecule into the carbon π^* band.

Recent work by Thomsen and Reich³³ using double-resonance theory, where the scattered intermediate and final states are actual electronic states, can be used to resolve the meaning of defects within NTs. This model was originally applied to one of the six-phonon branches of the dispersion relations of graphite from which we resolve the meaning of the D band. However, it is possible, and has been shown elsewhere, that this can also be applied to other dispersive phonon modes and can give a deeper insight into disorder effects.³⁴⁻⁴² Figure 3 shows normalized Raman spectra at different stages of the functionalization and shows two main characteristic first order peaks for the MWNTs.

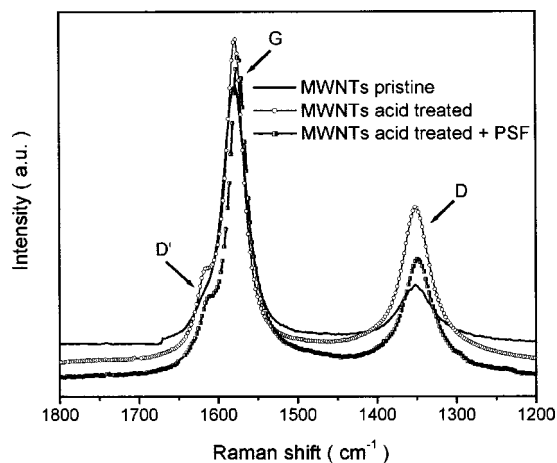


FIG. 3. Raman spectra of $--$ pristine MWNTs, $-\circ-$ MWNTs after acid treatment, and $-\square-$ MWNT after acid treatment and PSF dye. The D mode is the disorder-induced mode, the G mode is representative of the E_{2g} mode, and the D' mode is another disorder-induced mode, shown to be directly affected by disorder on the nanotube body.

First-order Raman spectra of the pristine sample show a very broad disorder-induced peak around 1350 cm^{-1} (D band) as the MWNTs have some concentration of lattice defects inherent in their structure. This peak arises due to different defect structures in MWNTs and finite-length effects; the breadth of this peak also reflects the inherent disorder with the entire sample. Initial acid treatment reduces amorphous defects; hence, we see a narrowing of the band. However, it also results in the nanotube body being attacked by the acid, introducing new defects along the tubular body. This increase in disorder is defect and functionalization related, and is distinguished from the amorphous carbon originally present.

Shown also in Fig. 3 is the G band located at the 1578 cm^{-1} for the untreated tubes, which is similar to that of graphite, and this position is directly linked to the tangential shear mode (E_{2g}).⁴³ Figure 3 also shows the prominent appearance of D' around 1617 cm^{-1} with acid treatment, a feature barely visible in the pristine tubes. The mode at 1617 cm^{-1} can be linked to extrema in the density of states (DOS) of MWNT.⁴³ There is a direct connection between the E_{2g} mode, the M -point zone edge mode, and the edge of the ΓK optical branch.⁴⁴ This mode is a consequence of defects along the tube body which affects the E_{2g} mode and so induces a strain. Consequently, as we alter the perfect two-dimensional (2D) graphitization to a more disordered structure by functionalization, a strain is introduced in the $C=C$ bond vibrations, which gives rise to the peak at 1617 cm^{-1} . Commonly, in materials containing bonds other than sp^2 , particularly in tetrahedral amorphous carbon ($ta-C$) or $ta-C:H$, a blueshift to as far as 1630 cm^{-1} , and in some cases to 1690 cm^{-1} (with 299 nm excitation), is seen.⁴⁵ This high peak position could only be due to short, strained $C=C$ bond stretching.⁴⁵

Introducing defects along the nanotube body in a controlled manner using acid treatment and using Raman spectroscopy to show that the vibrational response allows us to understand changes along the nanotube body.⁴⁶ Consequently, we see dramatic changes when PSF is introduced to the nanotubes. Upon introduction we see a change and decrease in the D' peak, a substantial shift by 5 cm^{-1} of the E_{2g} mode, and an increase in the D peak. The change in the D peak intensity is the same equivalent change in the D' peak intensity, corresponding to the PSF attaching to the dye.

As a consequence of "removing" the defects from the MWNT's using PSF attachment, we introduce further defects along the MWNT's body. This is seen as disorder as we no longer have a perfectly graphitized structure on the surface of the MWNTs, but one possessing dye attachments at positions of tubular defects; consequently, the MWNTs are functionalized by dye molecules. Adding PSF removes many of the acid-activated sites on the graphene outer layer of the MWNTs, as the MWNT outer layer attracts the PSF to the surface, and through self-assembly PSF-CNT functionalization occurs. This phenomenon is observed as a reduction in the intensity of the D' peak as the PSF sits on the acid-treated reactive sites of the nanotubes.

Atomic force microscopy (AFM) has gradually developed as an important tool to study carbon nanotubes.⁴⁷⁻⁵⁰

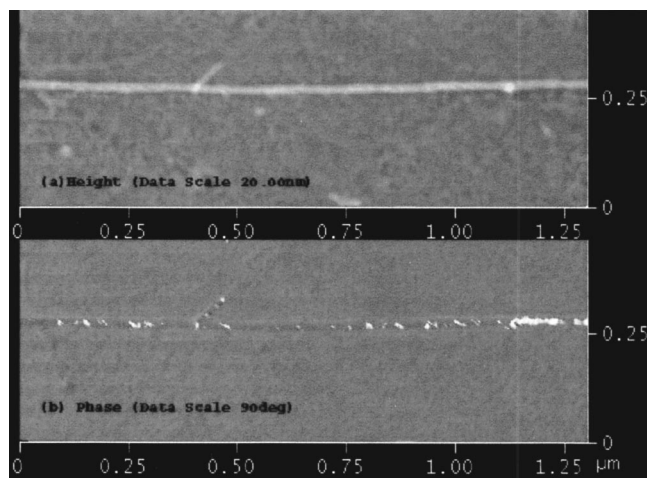


FIG. 4. AFM image of a single multiwalled nanotube with dye attachments on defect sites. (a) Height image (deflection) showing no apparent change in height on the locations of dye molecules (above). (b) Phase image showing clear contrast on regions of dye attachments at defect sites on the MWNT (below).

Phase imaging, in tapping mode, using an oscillating probe was employed to obtain nanometric images. This goes beyond topographic details to measure changes in surface properties like composition, adhesion, hardness, viscoelasticity, and more, by mapping the change in the phase of the cantilever oscillations. Samples for AFM measurements were prepared by drop-casting the solution of nanotubes dispersed in water onto a freshly cleaved highly oriented pyrolytic graphite (HOPG) substrate. This was then dried in air until the water has evaporated, leaving only nanotubes on the HOPG substrate. While no large change in topography could be observed at the sites of the dye attachment [Fig. 4(a)], attributed to the subnanometer size of the dye molecules, a more prominent contrast was detected in the phase image [Fig. 4(b)] at locations where the dye molecules were attached to defect sites on the nanotubes. This is as would be expected if the dye molecules in self-assembly attach only at CNT defect sites. In the phase image, minimal contrast is observed between the HOPG substrate and the multiwalled nanotubes owing to the similar graphitic nature of both materials. However, at locations where dye molecules are attached to the tube we can clearly see the PSF material present that is attached to the nanotube.

However, MWNT coverage is not complete as the PSF only adheres to acid-activated defect sites, and consequently we do not get aggregation of the dye on the entire length of the tube body.

In summary, our results show that phenosafranin (PSF) attaches to MWNT at acid-treatment-induced defects along the nanotube body. The attachment of the organic dye PSF was achieved through the process of self-assembly whereby the dye attaches on top of these induced defect sites. Spectroscopic verification using UV-visible and Raman spectroscopy showed a bathochromic shift in the UV-visible spectrum indicative of an electron transfer process between the nanotubes and PSF. In addition, we have spectroscopically fingerprinted the changes in the nanotube morphology due to self-assembly, indicated by changes in the D , G , and D'

vibrational position of the Raman spectra. Finally, using AFM, in tapping mode and phase image control, we were able to distinguish between the carbon nanotubes and the attached PSF. It is clear that the attachment was selective in that the only positions available for self-assembly attachment were at the defect sites. This advance in relatively simplistic self-assembly is an important one in that we can now start using organic molecules, in particular optoactive dyes, to alter the morphology and more concisely tailor the optical properties of nanotubes to meet more specific needs, optically, electronically, or biomedically.

We gratefully acknowledge funding from NSF-Nanoscale and Engineering Center at RPI.

- ¹M. A. Wilson, H. K. Patney, and J. Kalman, *Fuel* **81**, 5 (2002).
- ²A. G. Rinzler, J. Lui, H. Dai, P. Nikolaev, C. B. Huffman, F. J. Rodriguez-Macias, P. J. Boul, A. H. Lu, D. Heymann, D. T. Colbert, R. S. Lee, J. E. Fischer, A. M. Rao, P. C. Eklund, and R. E. Smalley, *Appl. Phys. A: Mater. Sci. Process.* **67**, 29 (1998).
- ³W. A. de Heer, A. Chatelain, and D. Ugarte, *Science* **270**, 1179 (1995).
- ⁴S. A. Curran, P. M. Ajayan, W. J. Blau, D. L. Carroll, J. N. Coleman, A. B. Dalton, A. P. Davey, A. Drury, B. McCarthy, S. Maier, and A. Strevens, *Adv. Mater. (Weinheim, Ger.)* **10**, 1091 (1998).
- ⁵S. Roth, S. Blumentritt, M. Burghard, E. Cammi, D. Carrol, S. Curran, G. Düsberg, K. Liu, J. Muster, G. Philipp, and T. Rabenau, *Synth. Met.* **94**, 105 (1998).
- ⁶K. Jiang, A. Eitan, L. S. Schadler, P. M. Ajayan, and R. W. Siegel, *Nano Lett.* **3**, 275 (2003).
- ⁷A. V. Ellis, K. Vijayamohan, R. Goswami, N. Chakrapani, L. S. Ramanathan, P. M. Ajayan, and G. Ramanath, *Nano Lett.* **3**, 279 (2003).
- ⁸R. K. Saini, I. W. Chiang, H. Peng, R. E. Smalley, W. E. Billups, R. H. Hauge, and J. L. Margrave, *J. Am. Chem. Soc.* **125**, 3617 (2003).
- ⁹V. Georgakilas, K. Kordatos, M. Prato, D. M. Guldi, M. Holzinger, and A. Hirsch, *J. Am. Chem. Soc.* **124**, 760 (2002).
- ¹⁰S. J. Tans, A. R. M. Verschueren, and C. Dekker, *Nature (London)* **393**, 49 (1998).
- ¹¹H. W. Ch. Postma, T. Teepen, Z. Yao, M. Grifoni, and C. Dekker, *Science* **293**, 76 (2001).
- ¹²Z. Yao, H. W. Ch. Postma, L. Balents, and C. Dekker, *Nature (London)* **402**, 273 (1999).
- ¹³R. D. Antonov and A. T. Johnson, *Phys. Rev. Lett.* **83**, 3274 (1999).
- ¹⁴C. Zhou, K. Jing, E. Yenilmez, and H. Dai, *Science* **290**, 1552 (2000).
- ¹⁵T. Rueckes, K. Kim, E. Joselevich, G. Y. Tseng, C. Cheung, and C. M. Lieber, *Science* **289**, 94 (2000).
- ¹⁶A. Bachtold, P. Hadley, T. Nakanishi, and C. Dekker, *Science* **294**, 1317 (2001).
- ¹⁷V. Derycke, R. Martel, J. Appenzeller, and Ph. Avouris, *Nano Lett.* **1**, 453 (2001).
- ¹⁸D. J. Hornbaker, S.-J. Kahng, S. Misra, B. W. Smith, A. T. Johnson, E. J. Mele, D. E. Luzzi, and A. Yazdani, *Science* **295**, 824 (2002).
- ¹⁹V. Lordi, N. Yao, and J. Wei, *Chem. Mater.* **13**, 733 (2001).
- ²⁰B. R. Azamian, K. S. Coleman, J. J. Davis, N. Hanson, and M. L. H. Green, *Chem. Commun. (Cambridge)* **2002**, 366 (2002).
- ²¹S. Banerjee and S. S. Wong, *J. Am. Chem. Soc.* **124**, 8940 (2002).
- ²²S. Banerjee and S. S. Wong, *Nano Lett.* **2**, 49 (2002).
- ²³Y. Li, C. Xu, B. Wei, X. Zhang, M. Zheng, D. Wu, and P. M. Ajayan, *Chem. Mater.* **14**, 483 (2002).
- ²⁴J. M. Planeix, N. Coustel, B. Coq, V. Brotons, P. S. Kumbhar, R. Dutartre, P. Geneste, P. Bernier, and P. M. J. Ajayan, *J. Am. Chem. Soc.* **116**, 7935 (1994).
- ²⁵B. C. Satishkumar, E. M. Vogl, A. Govindaraj, and C. N. R. Rao, *J. Appl. Phys.* **29**, 3173 (1996).
- ²⁶J. M. Haremza, M. A. Hahn, T. D. Krauss, S. Chen, and J. Calcines, *Nano Lett.* **2**, 1253 (2002).
- ²⁷J. Zhang, J.-K. Lee, Y. Wu, and R. W. Murray, *Nano Lett.* **3**, 403 (2003).
- ²⁸Y. Sun, S. R. Wilson, and D. I. Schuster, *J. Am. Chem. Soc.* **123**, 5348 (2001).
- ²⁹A. K. Jana, S. Roy, and B. B. Bhowmik, *Chem. Phys. Lett.* **168**, 365 (1990).
- ³⁰K. R. Gopidas and P. V. J. Kamat, *J. Photochem. Photobiol., A* **48**, 291 (1989).
- ³¹S. J. Boyer, *J. Chem. Phys.* **57**, 381 (1960).
- ³²A. M. Rao, P. C. Eklund, S. Bandow, A. Thess, and R. E. Smalley, *Nature (London)* **388**, 257 (1997).
- ³³C. Thomsen and S. Reich, *Phys. Rev. Lett.* **85**, 5214 (2000).
- ³⁴G. Samsonidze, R. Saito, A. Jorio, A. Souza Filho, G. M. A. Pimenta, G. Dresselhaus, and M. S. Dresselhaus, *Phys. Rev. Lett.* **90**, 027403 (2003).
- ³⁵R. Saito, A. Jorio, A. G. Souza Filho, G. Dresselhaus, M. S. Dresselhaus, and M. A. Pimenta, *Phys. Rev. Lett.* **88**, 027401 (2002).
- ³⁶I. Pócsik, M. Hundhausen, M. Koós, and Ley Lothar, *J. Non-Cryst. Solids* **227**, (1998).
- ³⁷P. H. Tan, C. Y. Hu, J. Dong, W. Shen, and B. Zhang, *Phys. Rev. B* **64**, 214301 (2001).
- ³⁸P. H. Tan, Y. Deng, and Q. Zhao, *Phys. Rev. B* **58**, 5435 (1998).
- ³⁹Y. Kawashima and G. Katagiri, *Phys. Rev. B* **52**, 10 053 (1995).
- ⁴⁰Y. Kawashima and G. Katagiri, *Phys. Rev. B* **59**, 62 (1999).
- ⁴¹L. Alvarez, A. Righi, S. Rols, E. Anglaret, and J. L. Sauvajol, *Chem. Phys. Lett.* **320**, 441 (2000).
- ⁴²P. H. Tang and Y. Tang, *Appl. Phys. Lett.* **75**, 1524 (1999).
- ⁴³P. C. Eklund, J. M. Holden, and R. A. Jishi, *Carbon* **33**, 959 (1995).
- ⁴⁴R. A. Jishi and G. Dresselhaus, *Phys. Rev. B* **26**, 4514 (1982).
- ⁴⁵A. C. Ferrari, *Diamond Relat. Mater.* **11**, 1053 (2002).
- ⁴⁶N. Chakrapani, S. Curran, B. Q. Wei, P. M. Ajayan, A. Carrillo, and K. Kane, *J. Mater. Res.* **18**, 2515 (2003).
- ⁴⁷S. C. Tsang, P. de Oliveira, J. J. Davis, M. L. H. Green, and H. A. O. Hill, *Chem. Phys. Lett.* **249**, 413 (1996).
- ⁴⁸S. Decossas, G. Cappello, G. Poignant, L. Patrone, A. M. Bonnot, F. Comin, and J. Chevrier, *Europhys. Lett.* **53**, 742 (2001).
- ⁴⁹U. Hubler, P. Jess, H. P. Lang, H.-J. Guntherodt, J.-P. Salvetat, and B. Forrero, *Carbon* **36**, 697 (1998).
- ⁵⁰L. P. Biro, *Carbon Filaments and Nanotubes: Common Origins, Differing Applications*, NATO Science Series, Series E: Applied Sciences (Plenum, New York, 2001), Vol. 372, p. 255.